Impact of Oil Film Dynamics on the Performance of Aeroengine Plain Bearings

Senlin Liu[iD], Yu Wang[*][iD]

School of Mechanical Engineering, Xihua University, 611730 Chengdu, China

[*] Correspondence: Yu Wang (wangyu@mail.xhu.edu.cn)

Citation: S. L. Liu and Y. Wang, "Impact of oil film dynamics on the performance of aeroengine plain bearings," *Precis. Mech. Digit. Fabr.*, vol. 1, no. 1, pp. 24–30, 2024. https://doi.org/10.56578/pmdf010103.

Abstract: This investigation addresses the issue of premature failure or damage to bearing components in aeroengines, which often results from the release of dissolved gases in the lubricant due to environmental pressure changes during operation. Employing the three-dimensional Reynolds equation and focusing on an ideal lubricating oil, a lubrication model for the engine camshaft's oil film was developed. The formation and extent of gaseous voids within plain bearings were analyzed. The study systematically explored how fit clearance and lubricating oil viscosity influence oil film pressure and thickness. It was found that a reduced fit gap increases the oil film pressure gradient while decreasing the film's thickness. Additionally, although variations in lubricating oil viscosity do not affect the distribution of oil film thickness, they significantly impact the pressure exerted on the oil film, with higher viscosities leading to increased pressures. These findings provide essential theoretical guidance for the safety assessment of aeroengine plain bearings.

Keywords: Fit gap; Lubricating oil viscosity; Oil film pressure; Oil film thickness; Gaseous hole

1 Introduction

As aerospace technology advances, the performance demands on aeroengines, which are crucial for powering aircraft, are steadily increasing. The engine's lubrication system is engineered to distribute lubricating oil to every bearing and gear within the engine, minimizing friction among components. It also dissipates considerable heat via the circulation of the lubricating fluid, thereby guaranteeing the engine's long-term stability and ensuring the aircraft's safety and reliability [1]. In the engine, the sliding bearing supports the high-speed rotation of the rotor shaft. Bearing lubrication can effectively reduce the loss caused by resistance and achieve a better cooling effect [2]. The lubrication bearing is a critical component of engines; its lubrication efficiency influences the engine's operational state. Both the oil film pressure and oil film thickness are pivotal in determining the lubrication effectiveness of plain bearings [3]. Consequently, studying the lubrication characteristics, oil film pressure, and oil film thickness of plain bearings is essential.

Allen and Raeymaekers [4] utilized a soft elastohydrodynamic lubrication model to explore microstructures and found that maximum oil film thickness occurs with tissue densities between 10% and 40% and texture ratios between 1% and 14%. They noted that in full oil film lubrication, film thickness is largely independent of the bearing surface's stiffness. Currently, research on oil film thickness primarily employs numerical calculations. By formulating dynamic equations for lubricating oil, researchers study variations in oil film thickness and pressure under different conditions and loads. Additionally, some scholars apply the Reynolds equation to examine bearing lubrication characteristics [5–8]. Typically, bearing dynamics research initially focuses on determining the pressure of the bearing oil film, often investigated through solving the Navier-Stokes equation using CFD software [9–12]. Zi et al. [13] performed steady-state calculations on plain and step bearings using CFD software, addressing the inertia terms and viscosity changes traditionally neglected in the Reynolds equation. Dong et al. [14] assessed the effects of dynamic pressure and eccentricity on the static characteristics of bearings through studies on radial static pressure gas bearings. Chapkov et al. [15] conducted numerical simulations to determine the distribution of lubricating oil film thickness, finding that film thickness increases with rolling speed. Hu et al. [16] used the multiphase flow VOF method for numerical research on the oil-gas phase of oil-jet lubricated bearings, discovering uneven distribution of oil and gas, with the minimum oil volume fraction appearing near the nozzle's upstream side. Sakai et al. [17] explored

temperature distribution under transition and insufficient lubrication conditions using two-phase flow computational fluid dynamics, finding minimal heat generation by shear friction under transition lubrication with bearing and oil supply temperatures nearly identical. Under insufficient lubrication, air from the oil supply tank creates a circulating flow, cooling the bearing's side end and controlling the center temperature. Shirzadegan et al. [18] observed higher pressure and reduced film thickness during their analysis of the elastic hydrodynamic lubrication of CAM and roller self-tests, highlighting the importance of camshaft design in piston engines and lubrication characteristics study of plain bearings. Under ideal conditions, main factors influencing the bearing capacity of the lubricating oil film include bearing clearance and oil viscosity. However, under high-speed rotation, cavitation in the pressure oil film can occur, altering film thickness and bearing capacity along the circumference. Harry et al. [19] discussed cavitation phenomena in lubricating oil films using CFD software, analyzed thermal effects through fluid-structure coupling technology, and evaluated the influence of shaft locus on heat transfer. Thus, as the supporting medium in clearance lubrication, lubricating oil's viscosity is influenced by external factors such as heat, and due to shaft pressure, dissolved gases in the oil may escape, forming gaseous voids and impacting the lubrication characteristics of plain bearings.

This paper focuses on oil film pressure and thickness as its primary research subjects. It simulates the impact of varying fit clearances on the oil film pressure and thickness during high-speed rotation of plain bearings. Additionally, the study accounts for the effects of different lubricating oil viscosities. The model presented is designed to have universal applicability.

2 Numerical Model

2.1 Finite Element Model

The three-dimensional model of the oil film was established. Considering the cavitation of the oil film, the two ends of the oil film were considered to be connected with the atmosphere, and the air pressure was zero. The eccentricity between the rotating shaft and the journal was set at 0.6, the inner diameter of the rotating shaft was 26.18 mm, the length of the oil film was 30 mm, and the rotating speed was 1200 rpm. The parameters of different lubricating oils are shown in Table 1 and Figure 1.

Table 1. Different types of lubricating oil

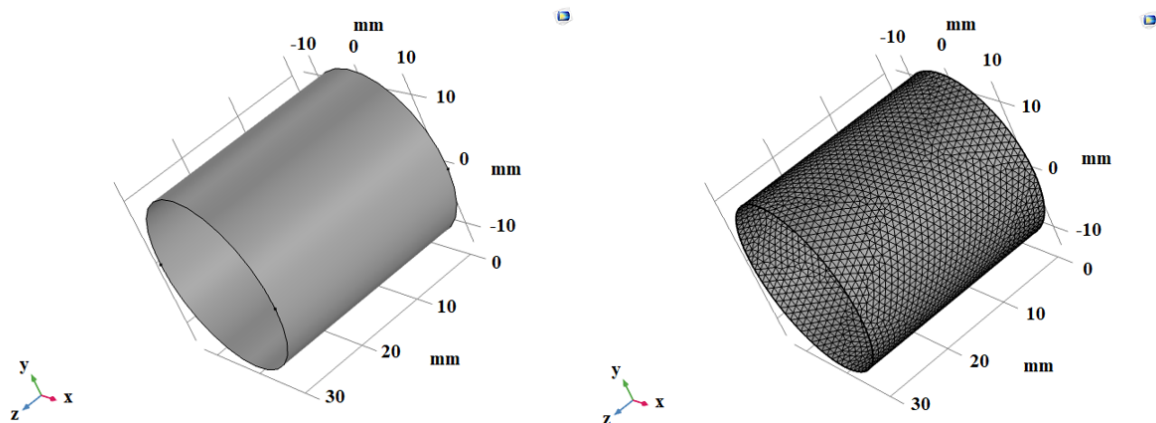| Lubricating Oil Type	SAE 5W-20	SAE 5W-30	SAE 10W-30	SAE 10W-40	SAE 20W-50
Density (g/ml)	0.859	0.859	0.858	0.867	0.874
ASTM D92	216	228	226		252
Kinematic viscosity $(\mathrm{mm^2/s})$	8.3	10.3	10.3	15.7	19.5
ASTM D97	-42	-39	-39	-39	-27
Dynamic viscosity (Pa.s)	0.0071297	0.0088477	0.0088374	0.0136119	0.017043

Figure 1. Finite element model for solving oil film pressure and thickness

2.2 Governing Equation

The pressure distribution inside the lubrication film is controlled by solving the time-dependent Reynolds equation, which controls the flow of Newtonian fluids at thin interfaces between relatively moving surfaces. For incompressible fluids without slip, the stationary Reynolds equation over a continuous range is given by:

$$\nabla_T \cdot \left(\frac{-\rho h^3}{12\mu} \nabla_T P + \frac{\rho h}{2} \left(v_a + v_b \right) \right) - \rho \left(\left(\nabla_T b \cdot v_b \right) - \left(\nabla_T a \cdot v_a \right) \right) = 0 \tag{1}$$

where, ρ represents the fluid density $\left(\mathrm{kg/m^3} \right)$, h represents the lubricant thickness (m), μ represents the dynamic viscosity of the fluid (Pa.s), p represents the pressure (Pa), a represents the inside diameter of the film (m), v_a represents the tangential velocity on the inside diameter $(\mathrm{m/s})$, b represents the outside diameter of the film (m), and v_k represents the tangential velocity on the inside diameter $(\mathrm{m/s})$.

The rotating journal is treated as a fixed wall in the model, with the assumption that the pressure remains constant across the entire thickness of the lubrication film. The gradient operator ∇_T is used to calculate the pressure distribution on the surface of the lubricant. In this case:

$$\rho \left(\left(\nabla_T b \cdot v_b \right) - \left(\nabla_T a \cdot v_a \right) \right) = 0 \tag{2}$$

$$\nabla_T \cdot \left(\frac{-\rho h^3}{12\mu} \nabla_T P + \frac{\rho h}{2} \left(v_a + v_b \right) \right) = 0 \tag{3}$$

In the established oil film lubrication model, the lubrication layer thickness h is defined as:

$$h = c(1 + \varepsilon \cos \theta) \tag{4}$$

where, $c = R_b - R_J$ represents the difference between the bearing radius and the journal radius, ε represents the eccentricity rate, and θ represents the polar coordinates of a point on the lubrication film.

The wedge gap between the bearing shell and the rotating shaft is the main geometric condition for the formation of dynamic pressure in oil film. There is a convergent wedge gap and an open wedge gap along the rotating shaft in the cylindrical bearing. One hypothesis [20] holds that there is a complete oil film in both wedges, that is, a full-circumference oil film (Sommerfeld boundary condition); the other hypothesis holds that there is a complete oil film in only convergent wedges, that is, a half-circumference oil film (half-Sommerfeld boundary condition). The Sommerfeld boundary condition is used in this paper. Under this boundary condition, negative pressure will appear in the calculation result of oil film pressure, which should be ignored in practice and considered as atmospheric pressure.

3 Result Analysis

The primary focus of this paper is divided into two main sections: the changes in oil film pressure and thickness under varying fit clearances and different types of lubricating oils, which are extensively discussed in this section.

3.1 Effect of Fit Gap

When the lubricating oil viscosity is 0.017Pa*s and the clearance c=0.05 mm, 0.1 mm, 0.1215 mm and 0.15 mm, the pressure distribution and thickness distribution on the oil film are calculated in Figure 2 and Figure 3.

As illustrated in Figure 2, the surface pressure of the oil film progressively declines as the fit gap increases. Owing to the eccentricity of the rotating shaft, there is a concentration of pressure on the surface of the oil film, resulting in an uneven distribution of surface pressure along the circumference of the oil film.

Figure 3 shows that the pressure distribution along the circumference of the oil film is uneven. This is attributed to the use of different oil film boundary models, resulting in a negative pressure area on the surface of the oil film, where the pressure is considered to be atmospheric. The surface pressure and thickness of the oil film decrease as the fit gap increases, with the oil film thickness peaking in the middle of the oil film circumference.

From the calculation and analysis, it is evident that the oil film thickness and pressure distribution are not uniform around the circumference of the oil film. The greatest deformation of the oil film occurs where it is thickest, and at this location, the pressure equals the environmental pressure. This pressure drops to or below the saturation pressure for the release of dissolved gases, leading to cavitation. The oil film thickness variation diagram indicates that larger fit clearances result in greater oil film deformation and reduced stability. Furthermore, combining the findings from both diagrams, we can conclude that smaller bearing clearances lead to thinner oil films, but the corresponding bearing capacity increases. Similarly, a smaller fit gap results in higher oil film pressure.
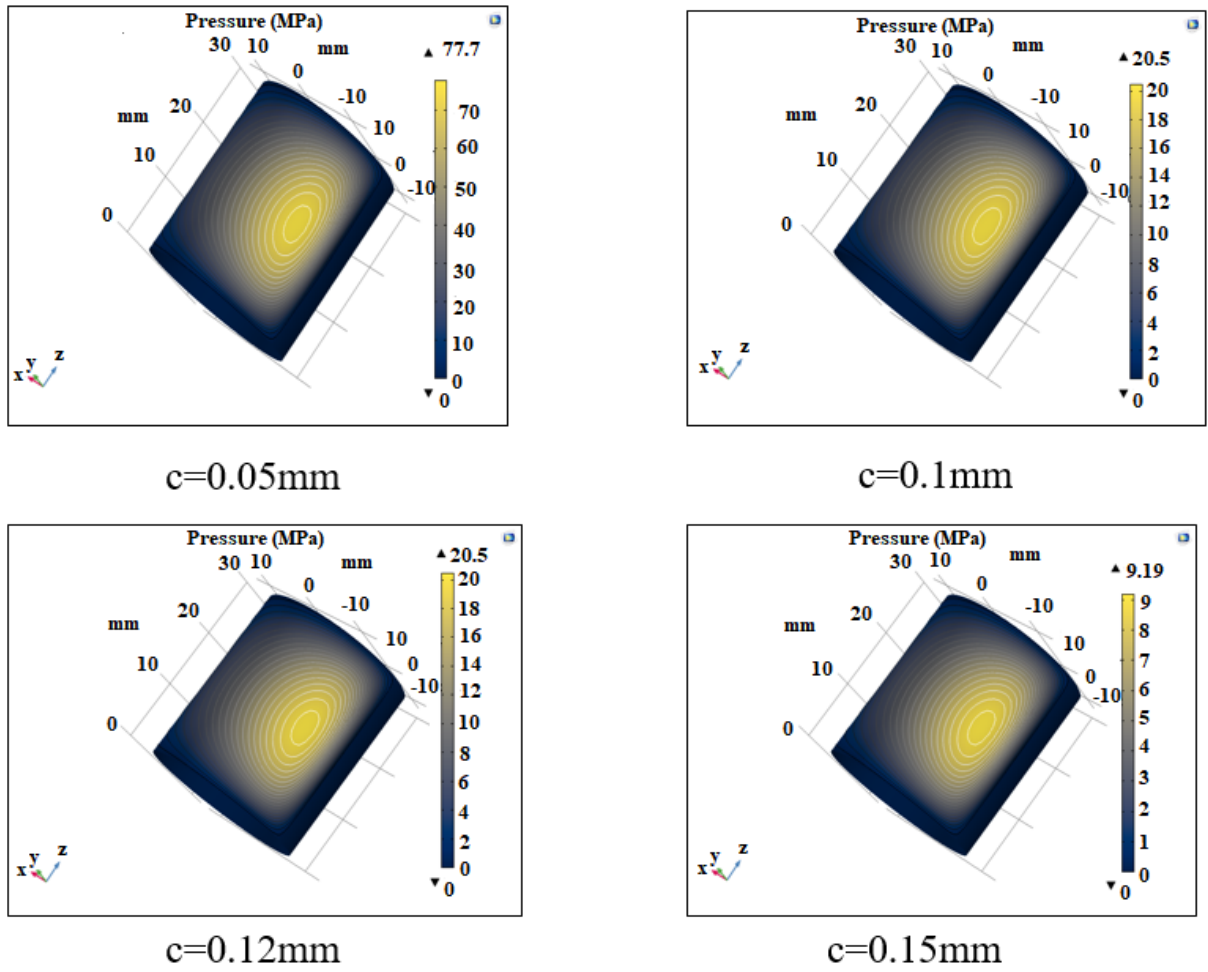
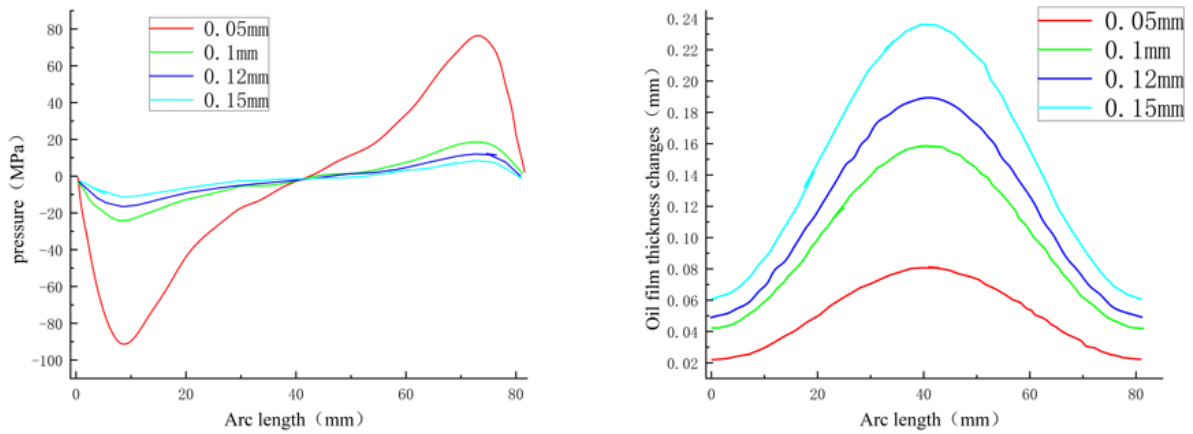**Figure 2.** Changes of oil film surface pressure

Figure 3. Changes of oil film pressure and thickness

3.2 Influence of Lubricating Oil Type

When oil flows within a confined space, the Marangoni effect, which arises from viscosity variations, also influences the oil's movement [21]. This section calculates the impact of oil viscosity on the lubrication system by examining the bearing capacity and film thickness effects of five different types of lubricating oils.

The governing equation for the pressure on the oil film remains the same as that used for the fit clearance calculations. Various types of lubricating oils are utilized to modulate the oil's viscosity as a controlled variable. This study investigates how different types of lubricating oil affect the surface pressure of the oil film. The viscosities of

these oils are detailed in Table 1. With a matching gap of c=0.05 mm, the resulting pressure distribution and thickness distribution on the oil film are presented as follows:
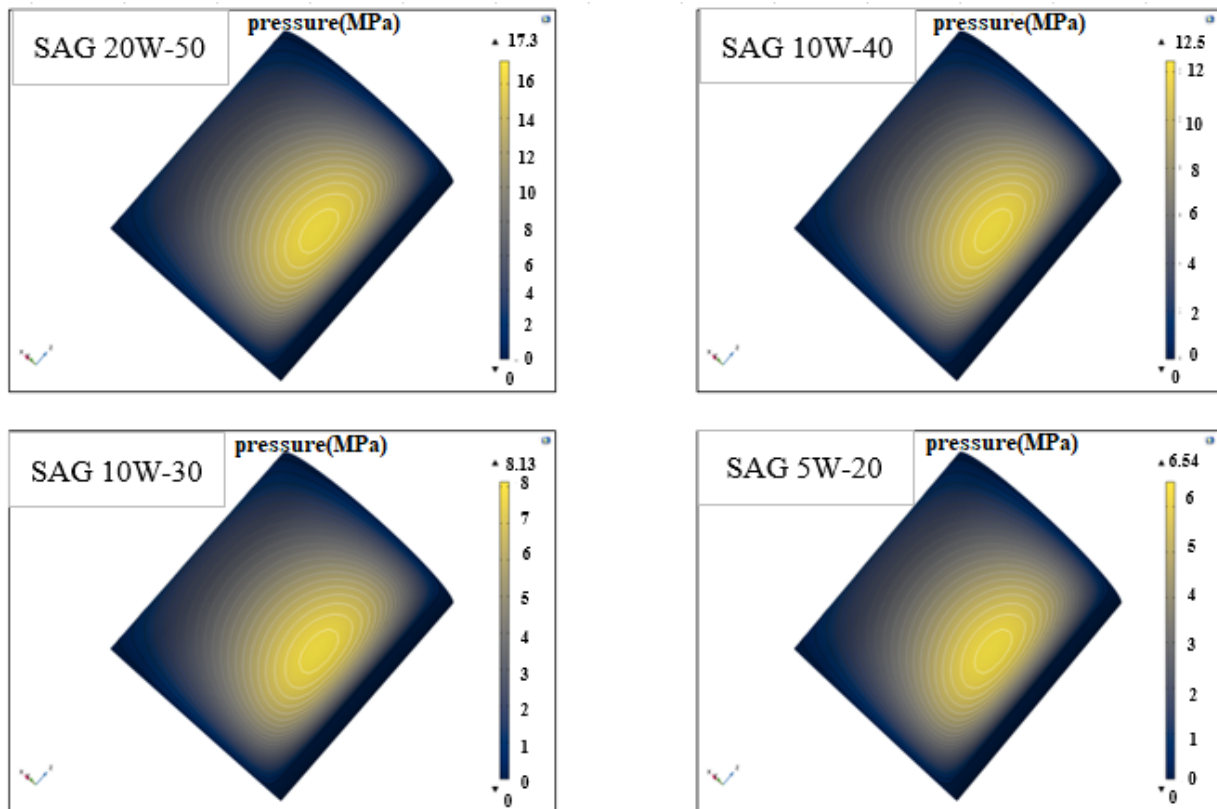

Figure 4. Changes of oil film pressure under the first 4 kinds of viscosity lubricating oil

Figure 4 demonstrates that as the viscosity of the lubricating oil increases, the pressure on the surface of the oil film also rises. Additionally, there is a localized concentration of pressure on the surface of the oil film, leading to an uneven pressure distribution along the circumference of the oil film.
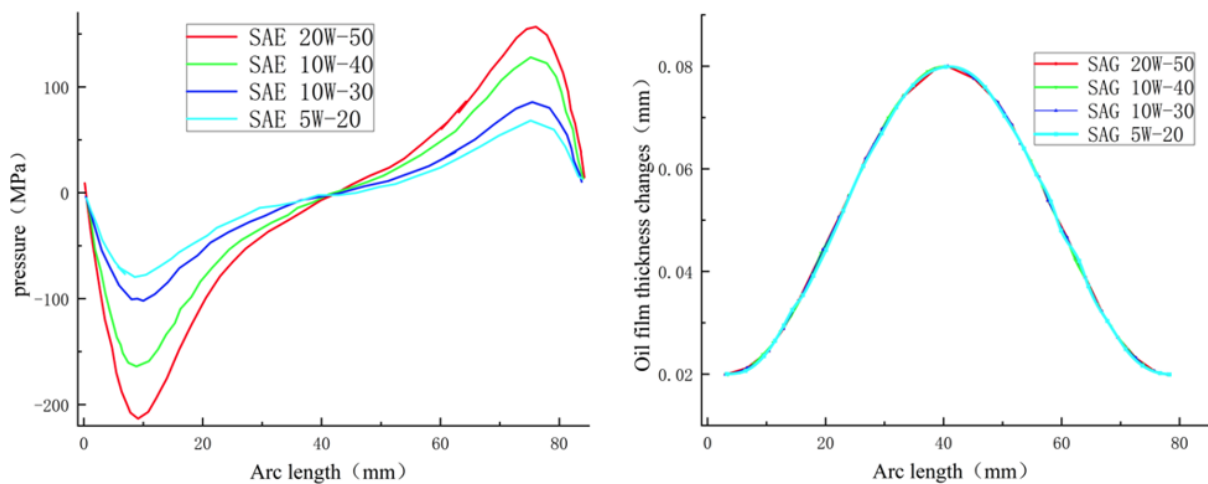

Figure 5. Changes of oil film pressure and thickness

As shown in Figure 5, the greater the viscosity of the lubricating oil, the higher the pressure on the surface of the oil film. However, the thickness of the oil film remains constant regardless of changes in oil viscosity. The maximum thickness of the oil film is located in the middle, while the highest pressure occurs near both sides.

The calculations also reveal that the thickness distribution of the oil film is uneven across its circumference, and variations in lubricating oil viscosity do not alter this uneven distribution. While the stability of the oil film remains

unchanged, viscosity influences the pressure exerted on the oil film. Higher viscosity results in increased surface pressure of the oil film.

4 Conclusions

This paper investigates the effects of fit clearance and lubricating oil type on the surface pressure and thickness distribution of the oil film. By solving the Reynolds equation in three dimensions and incorporating a switch function to manage the cavitation of the oil film, we have determined the variations in oil film pressure and thickness. The key findings are as follows:

(1) As the mating gap increases, the pressure on the surface of the oil film decreases, and there is a localized concentration of pressure near where cavitation of the oil film occurs.

(2) An increase in the viscosity of lubricating oil results in higher surface pressure of the oil film, although the thickness of the oil film remains unchanged.

Data Availability

The data used to support the research findings are available from the corresponding author upon request.

Conflicts of Interest

The authors declare no conflict of interest.

References

[1] A. Sinha, B. Brewster, K. Johnson, M. Walsh, and D. Hann, "How do interfacial shear and gravity affect the oil film characteristics near an aero-engine bearing?" *J. Eng. Gas Turbines Power*, vol. 144, no. 10, p. 101001, 2022. https://doi.org/10.1115/1.4055211

[2] P. Gloeckner and F. J. Ebert, "Micro-sliding in high-speed aircraft engine ball bearings," *Tribol. Trans.*, vol. 53, no. 3, pp. 369–375, 2010. https://doi.org/10.1080/10402000903312364

[3] J. Rooke, H. Brunskill, X. W. Li, S. Taghizadeh, A. Hunter, S. He, X. Q. Lu, and R. S. Dwyer-Joyce, "Piston ring oil film thickness measurements in a four-stroke diesel engine during steady-state, start-up and shut-down," *Int. J. Engine Res.*, vol. 24, no. 4, pp. 1499–1514, 2023. https://doi.org/10.1177/14680874221088547

[4] Q. Allen and B. Raeymaekers, "Maximizing the lubricant film thickness between a rigid microtextured and a smooth deformable surface in relative motion, using a soft elasto-hydrodynamic lubrication model," *J. Tribol.*, vol. 142, no. 7, p. 071802, 2020. https://doi.org/10.1115/1.4046291

[5] K. X. Pu, F. X. Yuan, P. C. Du, B. Huang, and D. D. Fei, "Study on influence of pad surface defects on lubrication characteristics of thrust bearing," *Ann. Nucl. Energy*, vol. 203, p. 110492, 2024. https://doi.org/10.1016/J.ANUCENE.2024.110492

[6] Y. Harigaya, M. Suzuki, F. Toda, and M. Takiguchi, "Analysis of oil film thickness and heat transfer on a piston ring of a diesel engine: Effect of lubricant viscosity," *J. Eng. Gas Turbines Power*, vol. 128, no. 3, pp. 685–693, 2006. https://doi.org/10.1115/1.1924403

[7] Y. Harigaya, M. Suzuki, and M. Takiguchi, "Analysis of oil film thickness on a piston ring of diesel engine: Effect of oil film temperature," *J. Eng. Gas Turbines Power*, vol. 125, no. 2, pp. 596–603, 2003. https://doi.org/10.1115/1.1501078

[8] F. Meng, Y. Zhang, Y. Hu, and H. Wang, "Thermo-elasto-hydrodynamic lubrication analysis of piston skirt considering oil film inertia effect," *Tribol. Int.*, vol. 40, no. 7, pp. 1089–1099, 2007. https://doi.org/10.1016/j.triboint.2006.10.006

[9] Y. F. Zhao, J. X. Yang, X. Ma, X. Y. Tie, and H. Q. Wang, "Effect of interface slip on friction of cylindrical pitted plain bearing," *Lubr. Seals*, vol. 44, no. 12, pp. 46–51, 2019. http://doi.org/10.3969/j.issn.0254-0150.2019.12.09

[10] J. W. Dong, H. B. Wen, J. C. Zhu, J. H. Guo, and C. Zong, "Analysis of thermo-hydrodynamic lubrication of three-lobe semi-floating ring bearing considering temperature–viscosity effect and static pressure flow," *Lubricants*, vol. 12, no. 4, p. 140, 2024. http://doi.org/10.3390/lubricants12040140

[11] X. D. Yu, Y. L. Lin, P. Wang, X. Y. Yang, Z. Y. Lan, M. J. Shao, L. Li, E. Z. Li, R. C. Dai, W. T. Jia, J. F. Wang, J. H. Jiao, and H. Jiang, "Analysis of lubrication characteristics of dynamic-static pressure hybrid thrust bearing considering key factors under eccentric loads," *Tribol. Int.*, vol. 194, p. 109471, 2024. https://doi.org/10.1016/j.triboint.2024.109471

[12] K. Budheeja and S. Verma, "Nonlinear transient analysis of hole-entry journal bearing with constant flow of micropolar fluids," *J. Mech. Eng. Sci.*, vol. 233, no. 1, pp. 350–368, 2019. https://doi.org/10.1177/0954406218756942

[13] X. T. Zi, K. Chen, Q. H. Bai, X. M. Li, X. Y. Jin, X. Wang, and F. Guo, "The enhancement of oil delivery and bearing performance via a guiding-structured nozzle under oil–air lubrication," *Lubricants*, vol. 12, no. 2, p. 60, 2024. https://doi.org/10.3390/lubricants12020060

[14] Y. H. Dong, Y. B. Niu, Y. Wang, G. Y. Li, and Y. H. Li, "Research on aerodynamic performance analysis of micro radial spiral-grooved air bearing," *Eng. Res. Express*, vol. 5, no. 1, p. 015001, 2023. https://doi.org/10.1088/2631-8695/acae20

[15] A. Chapkov, S. Bair, P. Cann, and A. Lubrecht, "Film thickness in point contacts under generalized Newtonian EHL conditions: Numerical and experimental analysis," *Tribol. Int.*, vol. 40, no. 10-12, pp. 1474–1478, 2007. https://doi.org/10.1016/j.triboint.2007.01.002

[16] J. B. Hu, W. Wu, M. X. Wu, and S. H. Yuan, "Numerical investigation of the air–oil two-phase flow inside an oil-jet lubricated ball bearing," *Int. J. Heat Mass Transfer*, vol. 68, pp. 85–93, 2014. https://doi.org/10.1016/j.ijheatmasstransfer.2013.09.013

[17] F. Sakai, M. Ochiai, and H. Hashimoto, "Two-phase flow CFD analysis of temperature effects on oil supplied to small-bore journal bearing with oil supply groove," *Tribol. Online*, vol. 13, no. 5, 2018. https://www.jstage.jst.go.jp/article/tribology/13/5/13_5/_article

[18] M. Shirzadegan, A. Almqvist, and R. Larsson, "Fully coupled EHL model for simulation of finite length line cam-roller follower contacts," *Tribol. Int.*, vol. 103, pp. 584–598, 2016. https://doi.org/10.1016/j.triboint.2016.08.017

[19] T. Harry, M. Zain, and S. Chhetri, "A confused patient with deranged liver function tests," *Pract. Neurol.*, vol. 20, no. 6, pp. 499–501, 2020. https://doi.org/10.1136/practneurol-2020-002594

[20] A. B. Shinde and P. M. Pawar, "Effect of partial grooving on the performance of hydrodynamic journal bearing," *Ind. Lubr. Tribol.*, vol. 69, no. 4, pp. 574–584, 2017. https://doi.org/10.1108/ILT-06-2016-0124

[21] T. W. Yang, H. H. Zhu, S. D. Fan, J. Wu, J. L. Yuan, and L. Y. Zheng, "Research on lubrication characteristics of ship stern bearings considering bearing installation errors," *Lubricants*, vol. 11, no. 11, p. 478, 2023. https://doi.org/10.3390/lubricants11110478